Supplementary Information

Supplementary Figures

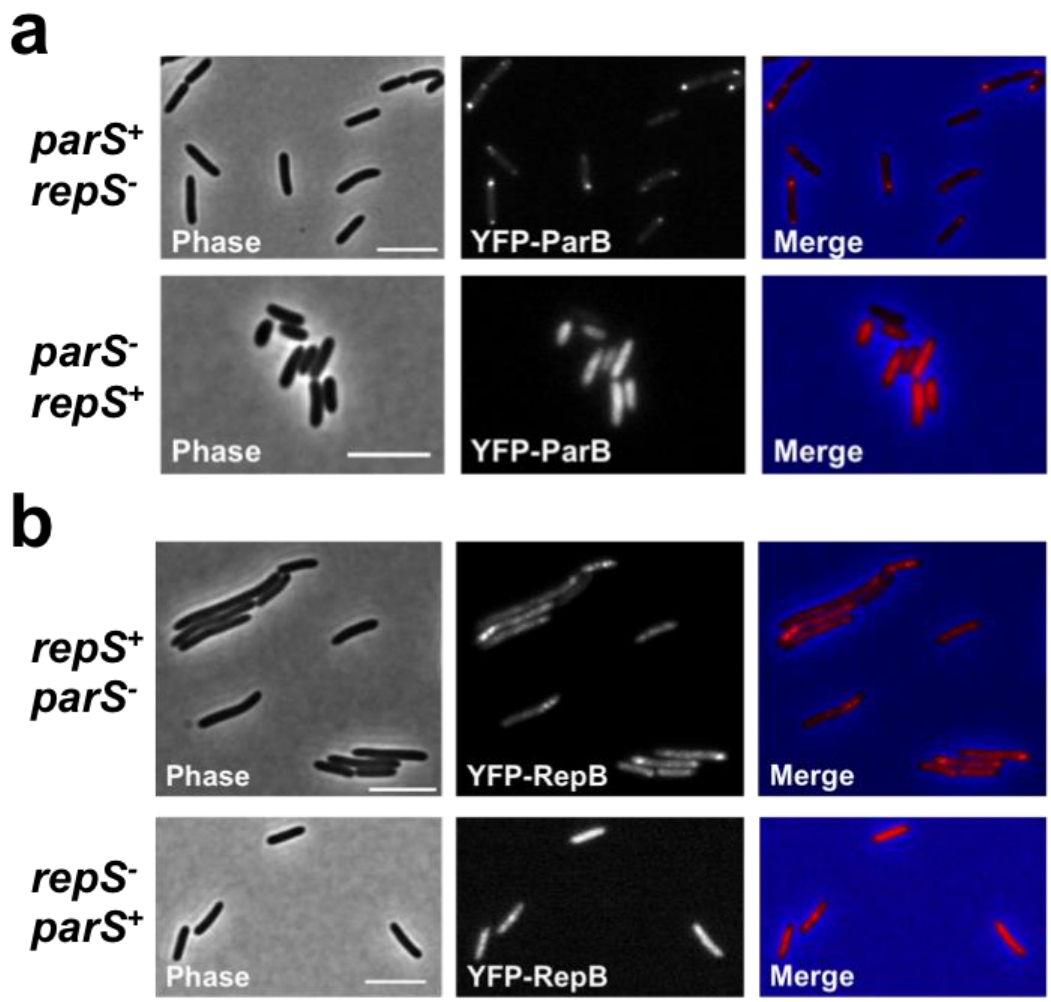

Supplementary Figure 1 | The presence of *parS* or *repS* influences the distribution of YFP-ParB and YFP-RepB fusions in *E. coli*. (**a**) YFP-ParB localization in *E. coli* STBL2 strain in the presence or absence of *B. abortus parS* sequence. When YFP-ParB is produced in a strain carrying a low copy number plasmid harboring a *parS* sequence, the YFP signal is expected to colocalize with the plasmid positions. (**b**) YFP-RepB localization in *E. coli* STBL2 strain in the presence or absence of *B. abortus repS* sequence. The distribution of the YFP-RepB signal is impacted by the presence of a plasmid carrying *repS* sequence. Scale bars represent 2 µm.

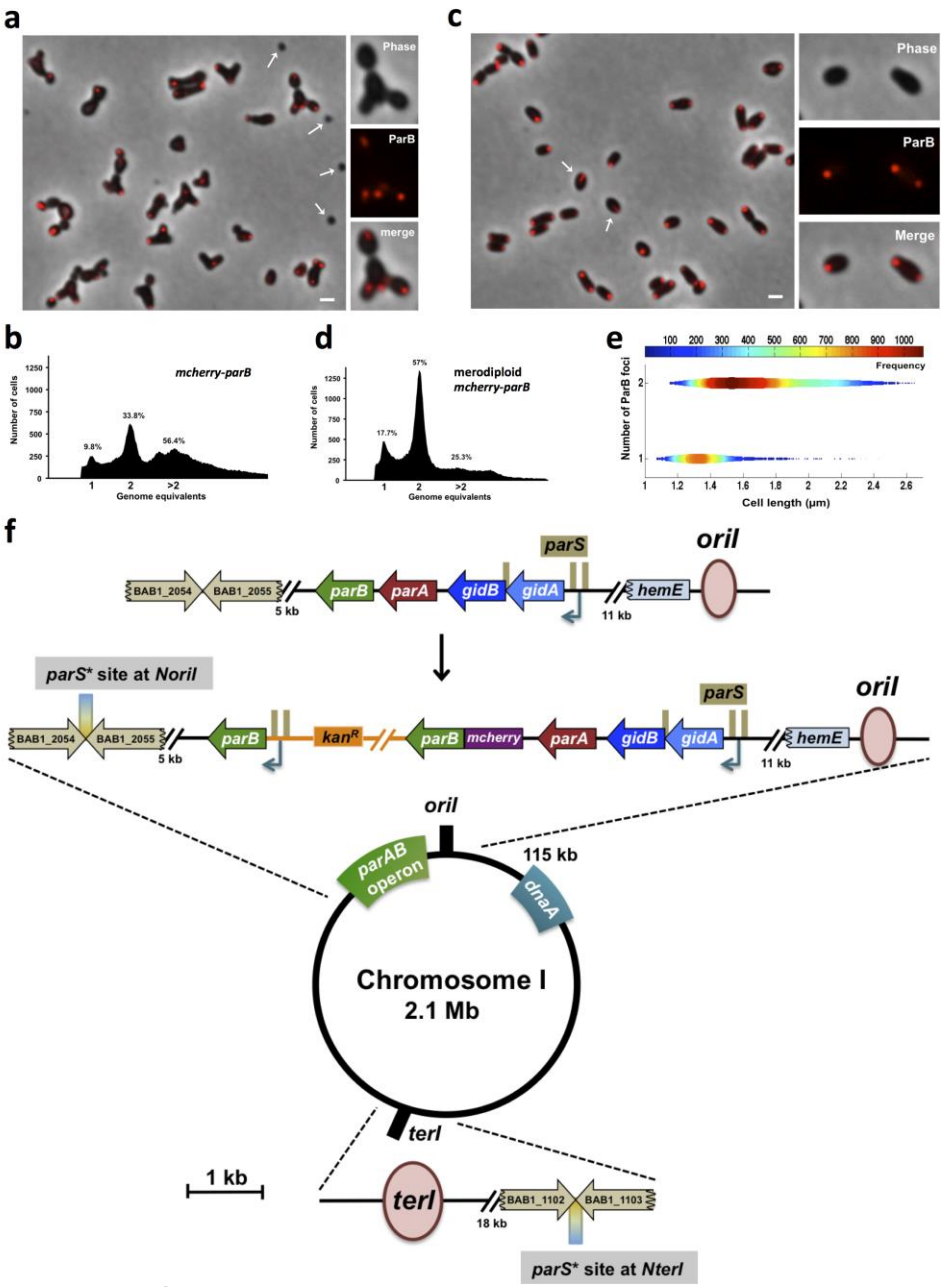

Supplementary Figure 2 | The mCherry-ParB fusion localizes at the cell poles. (**a**) mCherry-ParB (red) localization in a strain carrying *mcherry-parB* as the only copy of *parB* (*mcherry-parB* strain). Arrows indicate the presence of minicells. A large fraction of the population displays abnormal morphology and multiple mCherry-ParB foci. (**b**) Flow cytometry profile of the genomic content for the *mcherry-parB* strain showing a high proportion of more than 2n genome equivalent. (**c**) mCherry-ParB (red) localization in the merodiploid *mcherry-parB* strain carrying a copy of the untagged *parB* gene. Arrows point at two close foci indicating a recent duplication event of *oriI*. Scale bars in (a,c) represent 1 µm. (**d**) Flow cytometry profile of the genomic content for the merodiploid *mcherry-parB* strain showing a low proportion of more than 2n genome equivalent. (**e**) The bacterial population was sorted according to the number of ParB foci (one or two) and the frequency distribution for each subpopulation as a function of cell length is shown. (**f**) Map of the modifications made to chromosome I. The merodiploid *mcherry-parB* strain contains a *mcherry-parB* fusion at the *parABS* locus and an additional copy of *parB* under the control of the *gidA* promoter. The $parS_{P1}$ and $parS_{pMT1}$ sites are grouped under the *parS** name, which are inserted at the region neighboring *oriI* and *terI*, named *NoriI* and *NterI,* respectively.

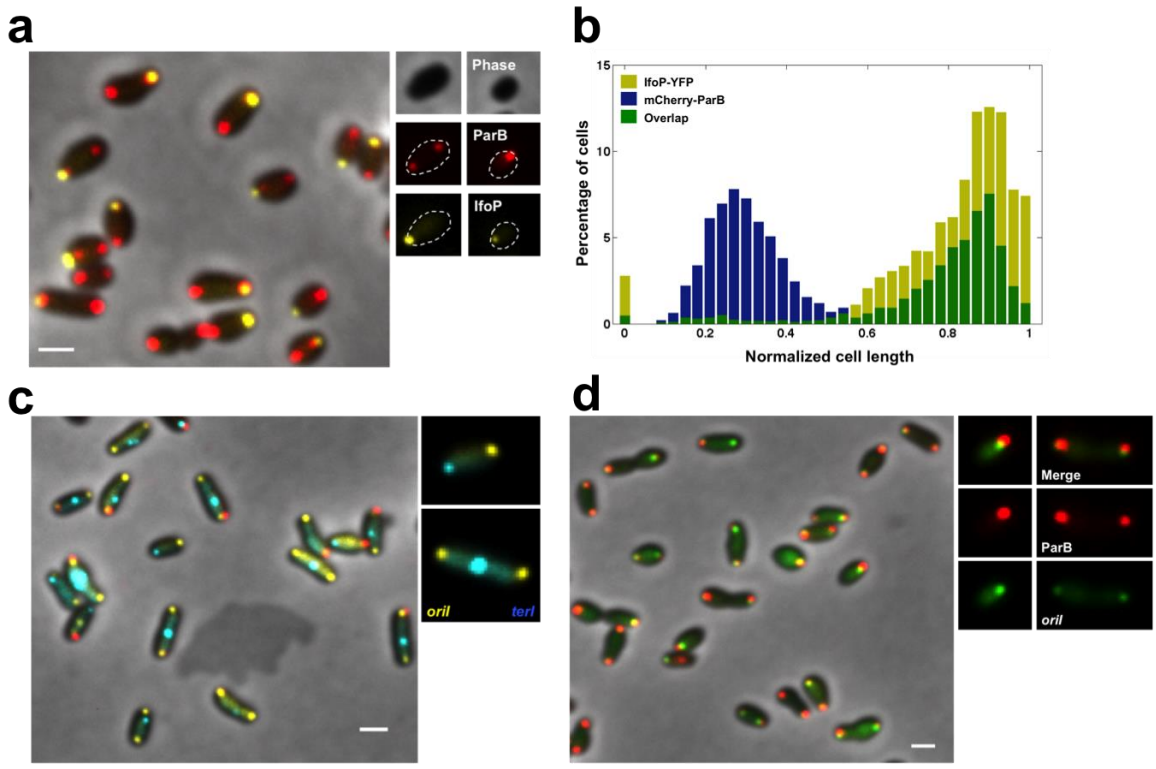

Supplementary Figure 3 | Chromosome I orientation. (**a**) Cells producing mCherry-ParB (red) and the new-pole marker IfoP-YFP (yellow) (see Supplementary Fig. 4) fusions. Single cells displaying only one spot of mCherry-ParB are found at the pole opposite to IfoP-YFP. (**b**) Histogram of the intracellular position of mCherry-ParB (blue) and IfoP-YFP (yellow) spots along a normalized cell length. In most cells, the duplicated mCherry-ParB focus occupies the same region as the new-pole marker IfoP-YFP. A low proportion of bacteria exhibits a pattern of localization where one mCherry-ParB focus is located at the old pole (at a normalized cell length of about 0.25) while the duplicated one occupies variable non-polar regions. This pattern is interpreted as a migration of the duplicated foci towards the new pole as previously reported for *C. crescentus*. (**c**) Cells producing *NoriI*-targeted YFP (yellow), *NterI*-targeted CFP (blue) and the old-pole marker PdhS-mCherry (red). (**d**) Colocalization between mCherry-ParB (red) and *NoriI*-targeted YFP (green). Scale bars represent 1 µm.

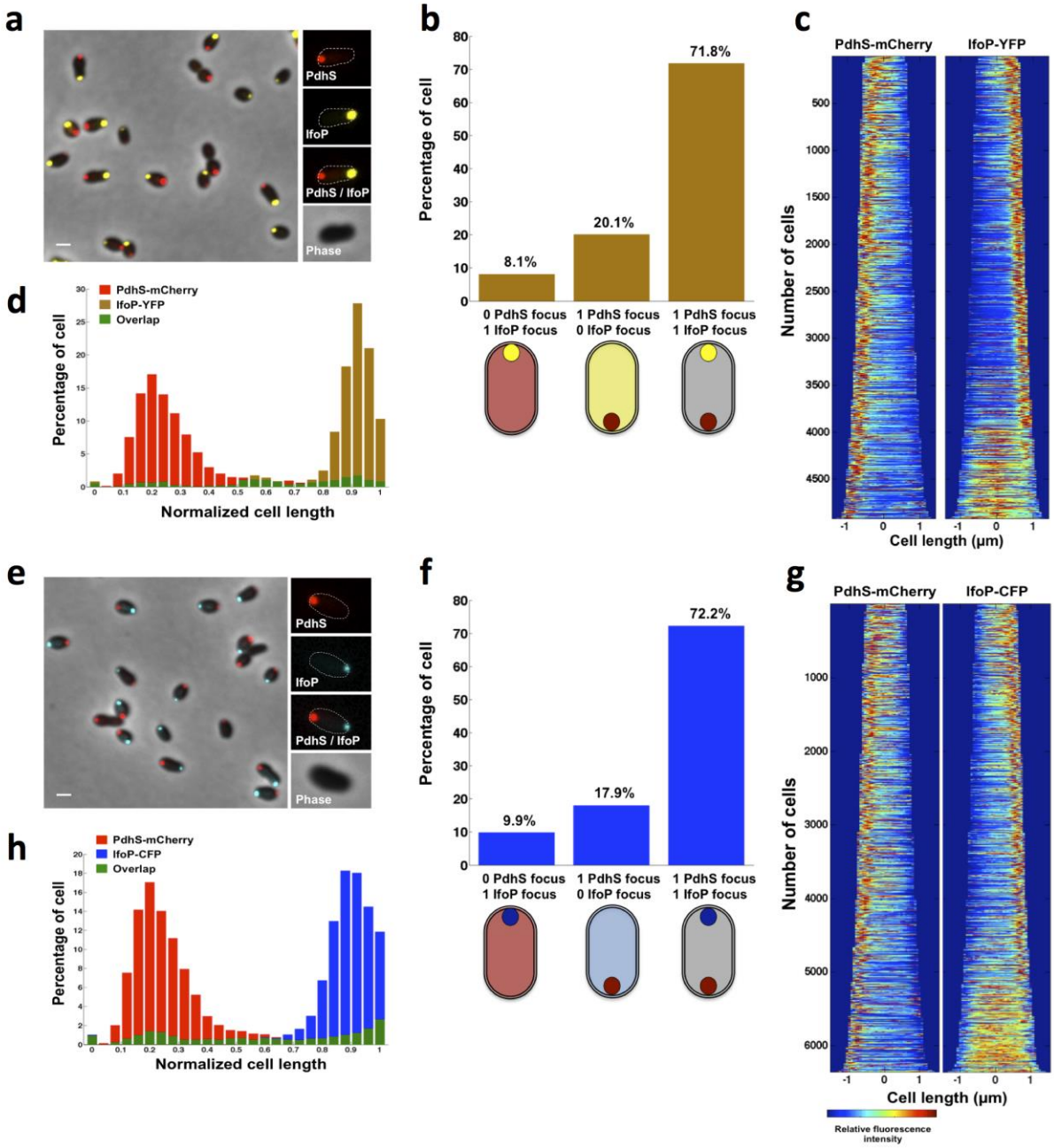

Supplementary Figure 4 | IfoP is a new pole marker in *B. abortus*. IfoP-CFP (XDB002) and IfoP-YFP (XDB005) fusions in *B. abortus.* (**a** and **e**) Cells showing localization of PdhS-mCherry (red) with either IfoP-YFP (yellow) or IfoP-CFP (blue) fusions. The IfoP spot is located at pole opposite to PdhS-mCherry except in the larger bacteria, in which IfoP is diffuse. Scale bar represents 1 µm. (**b** and **f**) Proportions of bacteria displaying different combinations of PdhS-mCherry and IfoP-YFP or IfoP-CFP spots. (**c** and **g**) Demographic representation of a strain producing PdhS-mCherry and IfoP-YFP or IfoP-CFP fusions. (**d** and **h**) Foci positions of PdhS-mCherry (red) and IfoP-YFP (yellow) or IfoP-CFP (blue) showing that both fusions occupy opposite polar regions. Green is the overlap between both distributions (n=4917 cells for XDB002 or 6068 cells for XDB005). The description of IfoP identification and its characterization in *B. abortus* are reported in Supplementary Note 1.

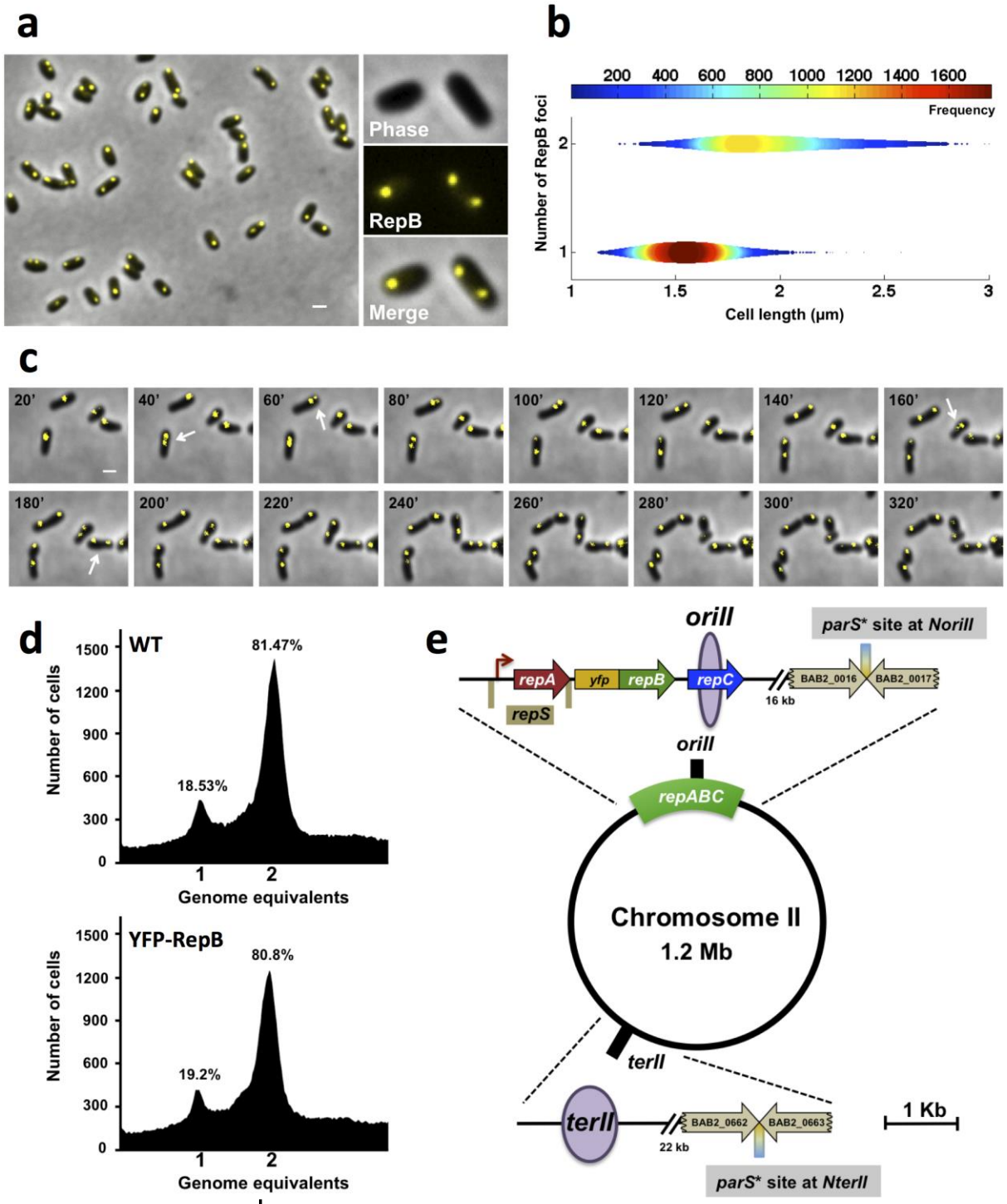

Supplementary Figure 5 | YFP-RepB is not attached to the poles. (**a**) Cells producing a YFP-RepB (yellow) fusion. (**b**) Frequency distribution of the population as a function of cell length for bacteria sorted according to the number of RepB foci (1 or 2). (**c**) Successive microscopy images of *B. abortus yfp-repB* strain from a time-lapse experiment. Displayed images were taken every 20 minutes. Arrows indicate YFP-RepB duplication events. (**d**) Flow cytometry profile comparison between the wild type (WT) and *yfp-repB* strains showing no alteration of genome equivalents. (**e**) Map of modifications made to chromosome II. The *yfp-repB* strain contains a *yfp-repB* fusion at the *repB* locus. The $parS_{P1}$ and $parS_{pMT1}$ sites are grouped under the *parS** name, and are inserted at the region neighboring to *oriI* and *terII*, termed *NoriII* and *NterII,* respectively.

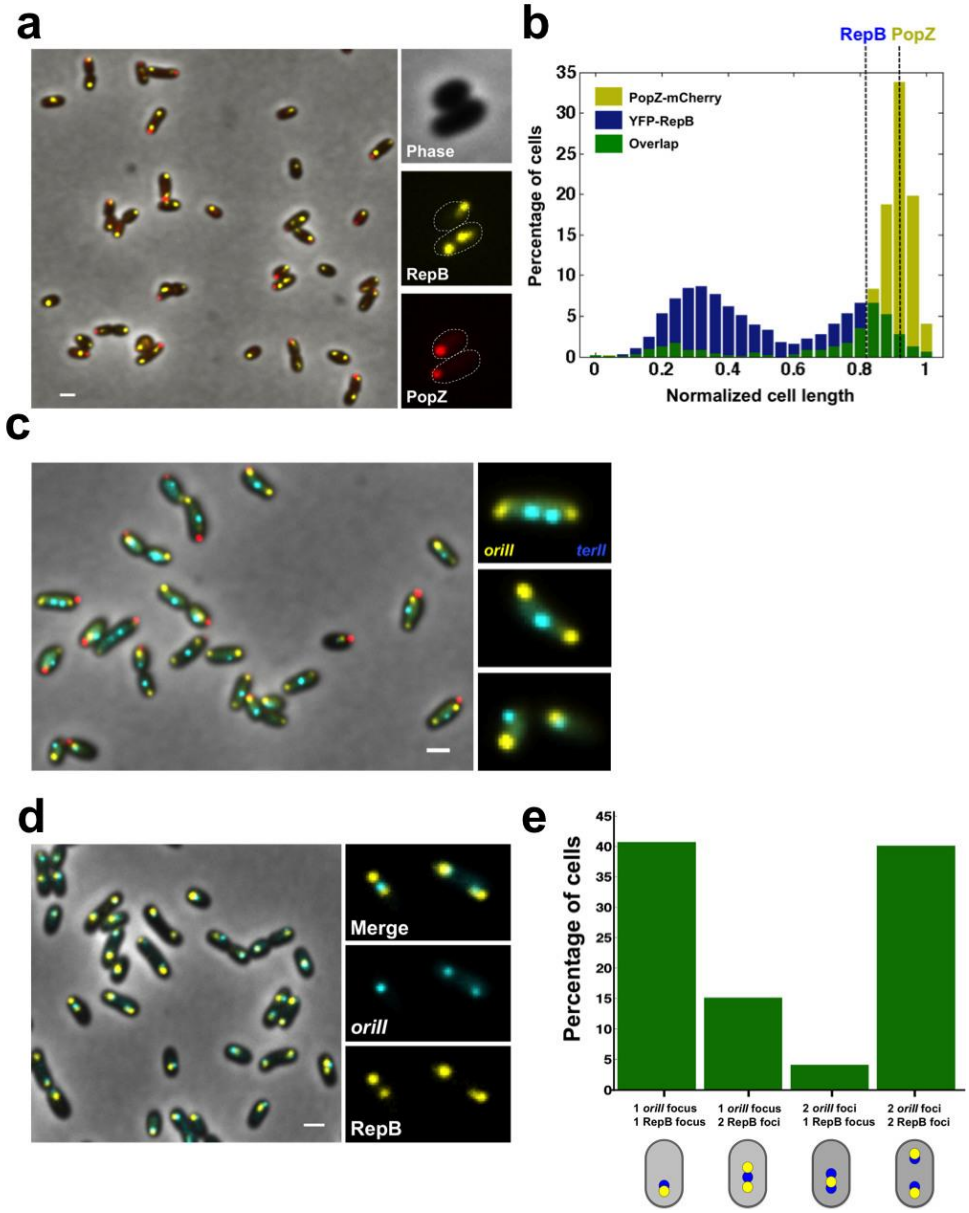

Supplementary Figure 6 | Chromosome II orientation. (**a**) Cells producing YFP-RepB (yellow) and the new-pole marker PopZ-mCherry (red) fusions (See Supplementary Fig. 7). (**b**) Histogram of the intracellular position of YFP-RepB (blue) and PopZ-mCherry (yellow) spots along a normalized cell length. Dashed lines represent modal frequencies of new pole proximal YFP-RepB and PopZ-mCherry foci position showing that RepB is less polar than PopZ. (**c**) Cells producing YFP-labeled *NoriII* (yellow), CFP-labeled *NterII* (blue) and the old-pole marker PdhS-mCherry (red). (**d**) Colocalization between YFP-RepB (yellow) and CFP-labeled *NoriII* (blue). (**e**) Fraction of cells with different combinations of YFP-RepB (yellow) and CFP-labeled *NoriII* spots for the different combinations. Only a few bacteria display a duplicated CFP-labeled *NoriII* focus and only one focus of YFP-RepB suggesting that the *repS* sequence is duplicated before *NoriII* region. Scale bars represent 1 µm.

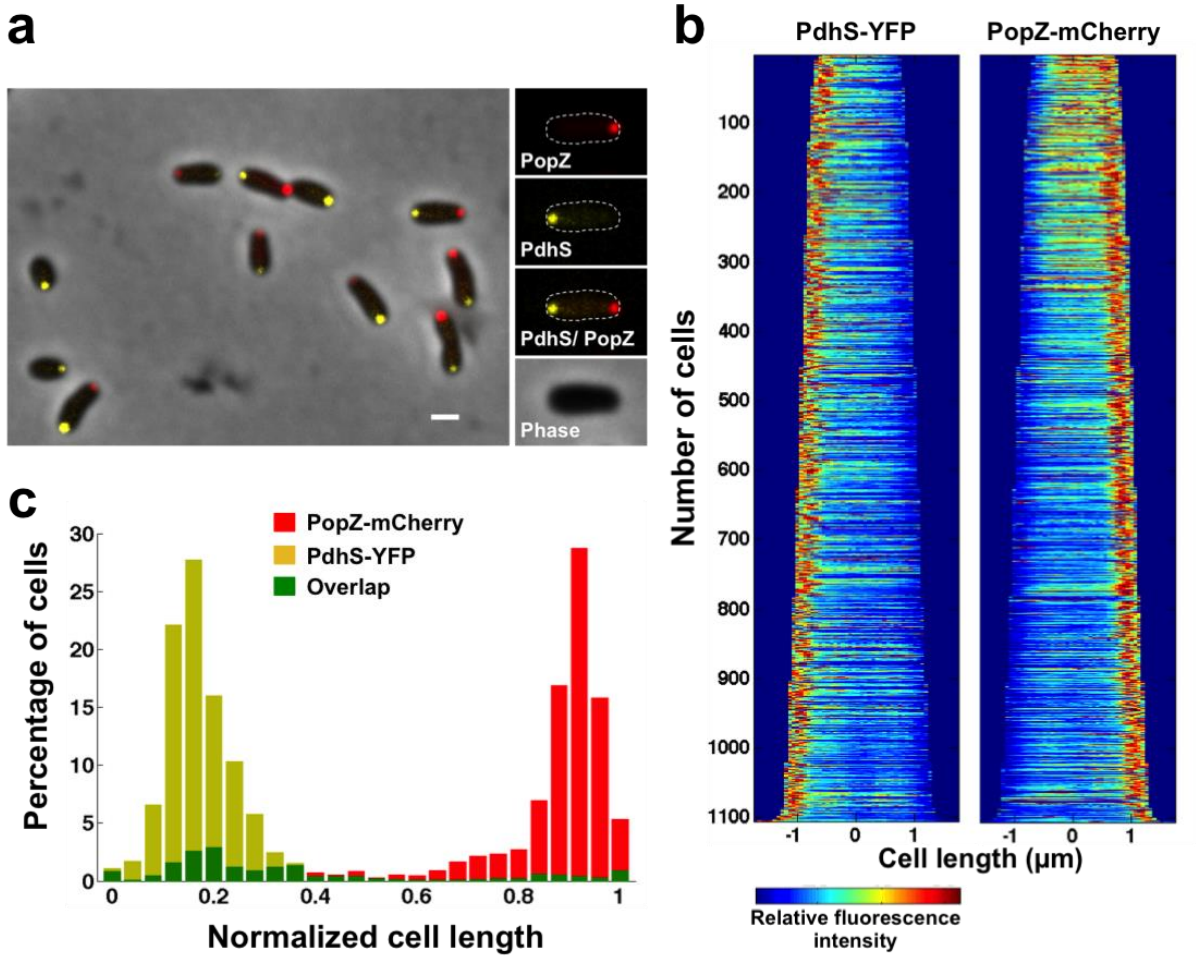

Supplementary Figure 7 | PopZ-mCherry localizes at the new pole in *B. abortus*. (**a**) Cells producing the old-pole marker PdhS-YFP (yellow) and PopZ-mCherry (red). PopZ-mCherry fusion is found at the pole opposite to PdhS-YFP. Scale bar represents 1 μm. (**b**) Demographic representation of PdhS-YFP and PopZ-mCherry fusions in cells displaying one focus of each fusion. (**c**) Intracellular position of PdhS-YFP (yellow) and PopZ-mCherry (red) spots along a normalized cell length. The two fusions occupy the opposite poles of the cells.

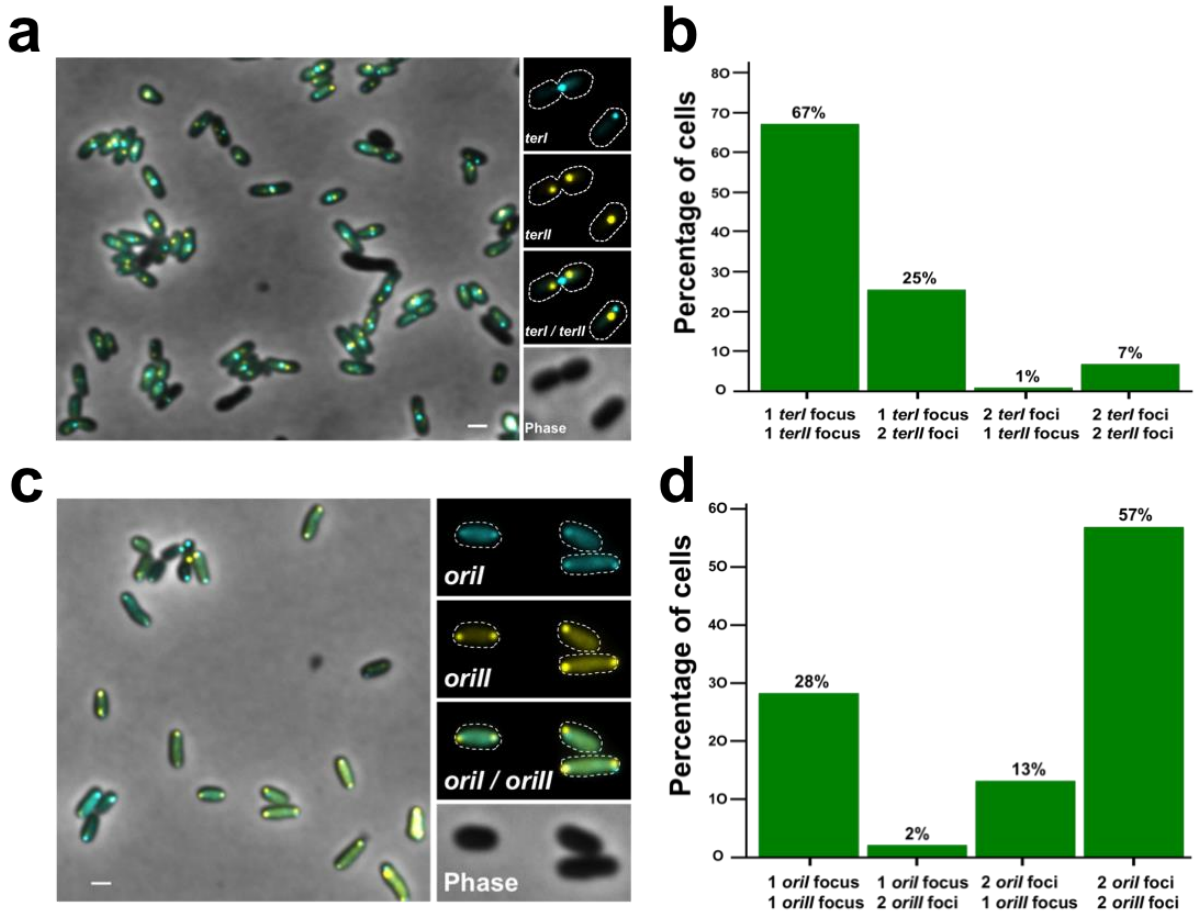

Supplementary Figure 8 | *NterII* is duplicated before *NterI* and *NoriI* is duplicated before *NoriII*. (**a**) Cells producing *NterI*-targeted CFP (blue) and *NterII*-targeted YFP (yellow) show one or two foci per terminator region despite variability in the levels of CFP-ParB$_{P1}$ and YFP-ParB$_{pMT1}$ signals between bacteria. Scale bars represent 1 µm. (**b**) Proportion of cells for different combinations of *NterI*-targeted CFP and *NterII*-targeted YFP spots. Almost no bacteria displaying one *NterII*-targeted YFP but only two *NterI*-targeted CFP spots are detected suggesting that segregation of chromosome II is completed before the one of chromosome I (n= 1305 cells). (**c**) Cells producing *NoriI*-targeted CFP (blue) and *NoriII*-targeted YFP (yellow) show the usual one or two foci distribution despite a variability in the levels of CFP-ParB$_{P1}$ and YFP-ParB$_{pMT1}$ signals between bacteria. (**d**) Proportion of cells for different combinations of *NoriI*-targeted CFP and *NoriII*-targeted YFP spots. Very few bacteria displaying two *NoriII*-targeted YFP but only one *NoriI*-targeted CFP spots are detected suggesting that replication initiation of chromosome I occurs before that of chromosome II (n=706 cells).

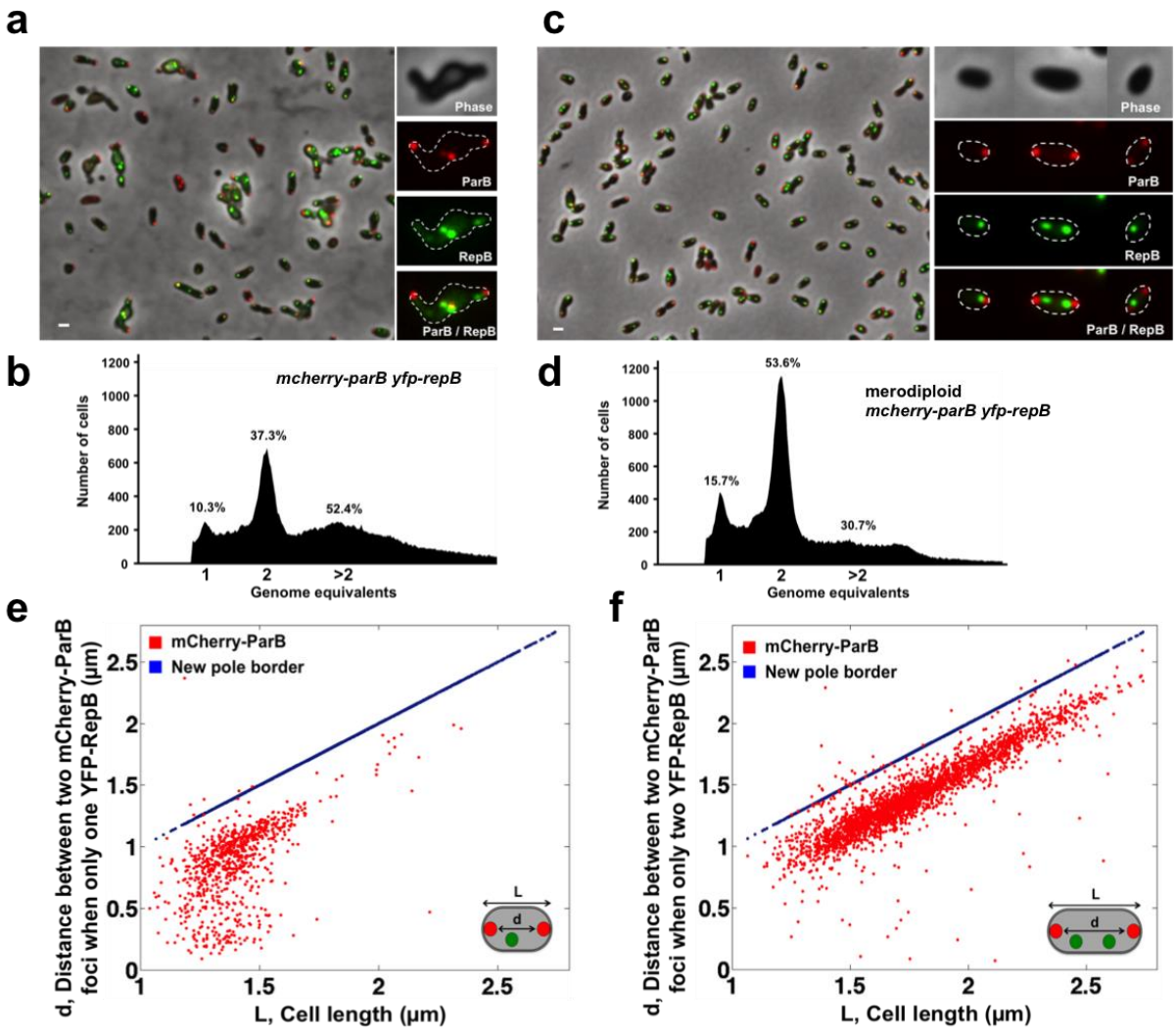

Supplementary Figure 9 | The YFP-RepB focus is duplicated after the mCherry-ParB focus. (**a**) Cells producing mCherry-ParB (red) and YFP-RepB (yellow) in *B. abortus mcherry-parB yfp-repB* strain (where *mcherry-parB* is the only allele of *parB*) showing branched and swelling cells. (**b**) Flow cytometry profile of the *mcherry-parB yfp-repB* strain shows a high proportion of abnormal genomic content (**c**) mCherry-ParB (red) and YFP-RepB (green) localization in the merodiploid *mcherry-parB yfp-repB* strain. Scale bars represent 1 µm. (**d**) Flow cytometry profile of the merodiploid *mcherry-parB yfp-repB* strain is similar to the wild-type strain. (**e**) Distance between two mCherry-ParB foci in the presence of a unique YFP-RepB. (**f**) Distance between two mCherry-ParB foci in the presence of two YFP-RepB indicating that YFP-RepB duplication occurred in bacteria displaying a strict bipolar localization of the mCherry-ParB fusion and not in bacteria in which the duplicated mCherry-ParB has not reach the growing pole yet.

Supplementary Tables

Supplementary Table 1. Strains used in this study

Strain name	Relevant genotype	Reference or source	Construction method	Specific feature
		***B. abortus* strain**		
XDB001	*Brucella abortus* 544	J.-M. Verger, INRA, Tours		
XDB002	*B. abortus pdhS*::pSK *kan pdhS-mcherry* /pMR *cat ifoP-cfp*	This study	Successive mating of XDB001 with S17-1 / pXDB020 (locus integration) and S17-1 / pXDB001	PdhS-mCherry / IfoP-CFP (new pole marker)
XDB003	*B. abortus parB::mcherry-parB*	This study	Mating between XDB001 and S17-1 / pXDB007 (allelic replacement)	mCherry-ParB (-)
XDB004	*B. abortus parB::mcherry-parB*-pSK *ori*T *kan PgidA-parB*	This study	Mating between XDB003 and S17-1 / pXDB008 (locus integration)	mCherry-ParB (+)
XDB005	*B. abortus parB::mcherry-parB*-pSK *ori*T *kan PgidA-parB* /pMR *cat ifop-yfp*	This study	Mating between XDB005 and S17-1 / pXDB009	mCherry-ParB (+) / IfoP-YFP (new pole marker)
XDB006	*B. abortus NoriI*::$parS_{pMT1}$ /pMR *kan yfp-*$parB_{pMT1}$ *cfp-*$parB_{P1}$	This study	Successive matings of XDB001 with S17-1 / pXDB011 (allelic replacement) and S17-1 / pXDB013	YFP-labeled *NoriI*
XDB007	*B. abortus NterI*::$parS_{P1}$ /pMR *kan yfp-*$parB_{pMT1}$ *cfp-*$parB_{P1}$	This study	Successive matings of XDB001 with S17-1 / pXDB012 (allelic replacement) and S17-1 / pXDB013	CFP-labeled *NterI*
XDB008	*B. abortus NoriI*::$parS_{pMT1}$ *NterI*::$parS_{P1}$ /pMR *kan yfp-*$parB_{pMT1}$ *cfp-*$parB_{P1}$	This study	Successive matings of XDB006 with S17-1 / pXDB012 (allelic replacement) and S17-1 / pXDB013	YFP-labeled *NoriI* / CFP-labeled *NterI*
XDB009	*B. abortus NoriI*::$parS_{pMT1}$ *NterI*::$parS_{P1}$ *pdhS*::pSK *kan pdhS-mcherry* /pMR	This study	Successive matings of XDB006 with S17-1 / pXDB012 (allelic replacement), S17-1 /	YFP-labeled *NoriI* / CFP-labeled *NterI* / PdhS-

	kan yfp-parB$_{pMT1}$ *cfp-parB*$_{P1}$		pXDB020 (locus integration) and S17-1 / pXDB013	mCherry (old pole marker)
XDB010	*B. abortus parB::mcherry-parB*-pSK *ori*T *kan PgidA-parB pdhS::*pSK *kan pdhS-mcherry NoriI::parS*$_{pMT1}$ /pMR *nours yfp-parB*$_{pMT1}$ *cfp-parB*$_{P1}$	This study	Successive matings of XDB003 with S17-1 / pXDB011 (allelic replacement), S17-1 / pXDB008 (locus integration) and S17-1 / pXDB013	mCherry-ParB (+) / YFP-labeled *NoriI*
XDB011	*B. abortus repB::yfp-repB*	This study	Mating between XDB001 and S17-1 / pXDB016 (allelic replacement)	YFP-RepB
XDB012	*B. abortus repB::yfp-repB popZ::*pKS *cat popZ-mcherry*	This study	Mating between XDB012 and S17-1 / pXDB017 (locus integration)	YFP-RepB / PopZ-mCherry (new pole marker)
XDB013	*B. abortus NoriII*::*parS*$_{pMT1}$ /pMR *kan yfp-parB*$_{pMT1}$ *cfp-parB*$_{P1}$	This study	Successive matings of XDB001 with S17-1 / pXDB018 (allelic replacement) and S17-1 / pXDB013	YFP-labeled *NoriII*
XDB014	*B. abortus NterII*::*parS*$_{P1}$ /pMR *kan yfp-parB*$_{pMT1}$ *cfp-parB*$_{P1}$	This study	Successive matings of XDB001 with S17-1 / pXDB019 (allelic replacement) and S17-1 / pXDB013	CFP-labeled *NterII*
XDB015	*B. abortus NoriII::parS*$_{pMT1}$ *NterII::parS*$_{P1}$ /pMR *kan yfp-parB*$_{pMT1}$ *cfp-parB*$_{P1}$	This study	Successive matings of XDB013 with S17-1 / pXDB019 (allelic replacement) and S17-1 / pXDB013	YFP-labeled *NoriII* / CFP-labeled *NterII*
XDB016	*B. abortus NoriII*::*parS*$_{pMT1}$ *NterII::parS*$_{P1}$ *pdhS::*pSK *kan pdhS-mcherry* /pMR *kan yfp-parB*$_{pMT1}$ *cfp-parB*$_{P1}$	This study	Successive matings of XDB013 with S17-1 / pXDB019 (allelic replacement), S17-1 / pXDB020 (locus integration) and S17-1 / pXDB013	YFP-labeled *NoriII* / CFP-labeled *NterII* / PdhS-mCherry (old pole marker)
XDB017	*B. abortus repB::yfp-repB NoriII::parS*$_{P1}$ /pMR *kan cfp-parB*$_{P1}$	This study	Successive matings of XDB011 with S17-1 / pXDB021 (allelic replacement) and S17-1 / pXDB015	YFP-RepB / CFP-labeled *NoriII*
XDB018	*B. abortus parB::mcherry-parB*	This study	Mating between XDB003 and S17-1 /	mCherry-ParB (-) /

	repB::yfp-repB		pXDB016 (allelic replacement)	YFP-RepB
XDB019	*B. abortus parB::mcherry-parB*-pSK *ori*T *kan PgidA-parB repB::yfp-repB*	This study	Successive matings of XDB003 with S17-1 / pXDB016 (allelic replacement) and S17-1 / pXDB008 (locus integration)	mCherry-ParB (+) / YFP-RepB
XDB020	*B. abortus NoriI*::$parS_{P1}$ *NoriII*::$parS_{pMT1}$ /pMR *nours yfp-*$parB_{pMT1}$ *cfp-*$parB_{P1}$	This study	Successive matings of XDB001 with S17-1 / pXDB010 (allelic replacement), S17-1 / pXDB018 (allelic replacement) and S17-1 / pXDB022	CFP-labeled *NoriI* / YFP-labeled *NoriII*
XDB021	*B. abortus NterI*::$parS_{P1}$ *NterII*::$parS_{pMT1}$ /pMR *nours yfp-*$parB_{pMT1}$ *cfp-*$parB_{P1}$	This study	Successive matings of XDB001 with S17-1 / pXDB012 (allelic replacement), S17-1 / pXDB019 (allelic replacement) and S17-1 / pXDB022	CFP-labeled *NterI* / YFP-labeled *NterII*
XDB022	*B. abortus parB::mcherry-parB*-pSK *ori*T *kan PgidA-parB pdhS::*pSK *kan pdhS-mcherry* /pBBR *cm PsojA-gfp*	This study	Mating between XDB004 and S17-1 / pXDB023	mCherry-ParB (+) / GFP
		***E. coli* strains**		
DH10B	F- *end*A1 *rec*A1 *gal*E15 *gal*K16 *nupG rpsL* Δ*lac*X74 Φ80*lac*ZΔM15 araD139 Δ(ara,leu)7697 mcrA Δ(mrr-hsdRMS-mcrBC) λ-; used for plasmids preparation	Invitrogen		
S17-1	M294::RP4-2 (Tc::Mu)(Km::Tn7); used for conjugative transfer (mating)	[2]		
STBL2	F- *end*A1 *gln*V44 *thi*-1 *rec*A1 *gyr*A96 *rel*A1 Δ(l*ac-proAB*) *mcrA* Δ(*mcrBC-hsdRMS-mrr*) λ-	Invitrogen		
XDB023	STBL2 /pBBR IBA3+ *yfp-parB*	This study	Transformation of STBL2 with pXDB002	YFP-ParB
XDB024	STBL2 /pBBR IBA3+	This	Transformation of	YFP-RepB

	yfp-repB	study	STBL2 with pXDB003	
XDB025	STBL2 /pBBR IBA3+ *yfp-parB* /pPR9TT *lacO parS1-2*	This study	Transformation of XDB022 with pXDB004	YFP-ParB (*parS*+)
XDB026	STBL2 /pBBR IBA3+ *yfp-parB* pPR9TT *lacO repS1*	This study	Transformation of XDB022 with pXDB005	YFP-ParB (*repS*+)
XDB027	STBL2 /pBBR IBA3+ *yfp-repB* /pPR9TT *lacO repS1*	This study	Transformation of XDB023 with pXDB005	YFP-RepB (*repS*+)
XDB028	STBL2 /pBBR IBA3+ *yfp-repB* /pPR9TT *lacO repS2*	This study	Transformation of XDB023 with pXDB006	YFP-RepB (*repS*+)
XDB029	STBL2 /pBBR IBA3+ *yfp-repB* /pPR9TT *lacO parS1-2*	This study	Transformation of XDB023 with pXDB004	YFP-RepB (*parS*+)

Supplementary Table 2. Plasmids used in this study

Plasmid number	Plasmid name	Reference
pXDB001	pMR *cat ifoP-cfp*	This study
pXDB002	pBBR IBA3+ *yfp-parB*	This study
pXDB003	pBBR IBA3+ *yfp-repB*	This study
pXDB004	pPR9TT *lacO parS1-2*	This study
pXDB005	pPR9TT *lacO repS1*	This study
pXDB006	pPR9TT *lacO repS2*	This study
pXDB007	pNPTS *mcherry-parB*	This study
pXDB008	pSK *ori*T *kan PgidA-parB*	This study
pXDB009	pMR *cat ifoP-yfp*	This study
pXDB010	pNPTS $NoriI_{P1}$	This study
pXDB011	pNPTS $NoriI_{pMT1}$	This study
pXDB012	pNPTS $NterI_{P1}$	This study
pXDB013	pMR *kan yfp-parB*$_{pMT1}$ *cfp-parB*$_{P1}$	This study
pXDB014	pMR *kan yfp-parB*$_{pMT1}$	This study
pXDB015	pMR *kan cfp-parB*$_{P1}$	This study
pXDB016	pNPTS *yfp-repB*	This study
pXDB017	pKS *ori*T *popZ-mcherry*	This study
pXDB018	pNPTS $NoriII_{pMT1}$	This study
pXDB019	pNPTS $NterII_{P1}$	This study
pXDB020	pSK *kan pdhS-mcherry*	[3]
pXDB021	pNPTS $NoriII_{P1}$	This study
pXDB022	pMR *nours yfp-parB*$_{pMT1}$ *cfp-parB*$_{P1}$	This study
pXDB023	pBBR *cm PsojA-gfp*	David Fretin, UNamur
pXDB024	pKS *ori*T *cat* $parS_{P1}$	This study
pXDB025	pKS *ori*T *cat* $parS_{pMT1}$	This study
pXDB026	pNPTS-t*parA-yfp-parB*	This study
pXDB027	pKS *ori*T *cat mcherry*	This study
pLAU43	pUC18-derivative KmR containing *lacO* arrays	[4]
pPR9TT	RK2-derivative	[5]
pNPTS 138	suicide plasmid for in-frame deletions, KanR	M. R. K. Alley, Imperial College of Science, London, UK
pSK *ori*T *kan*	pBluescript SK(-)-derived, bearing RP4 conjugative transfer origin oriT and kanamycine resistance marker *kan*	[6]

pKS *ori*T *cat*	pBluescript SK(-)-derived, bearing RP4 conjugative transfer origin oriT and chloramphenicol resistance marker cat	Isabelle Danese and Pascal Lestrate, UNamur
pMR *kan*	pMR10 (RK2*oriV*-derived) bearing kanamycine resistance marker *kan*	C.D. Mohr and R.C. Roberts, Stanford University
pBBR1 MCS1	Broad-host-range plasmid, KanR	[7]
pMR *nours*	pMR10-derived bearing kanamycine resistance marker *nours*	This study

Supplementary Table 3. Primers used in this study

Primer name	5'-3' primer sequence*
P1	aatgccagcacgggtct
P2	gctcaccatcgctcggcatattcctg
P3	tgccgagcgatggtgagcaagggcga
P4	ggGGATCCgcatcgTCTAGAggtggccgaccgcttgtacagctcgtccatgc
P5	ggGGATCCgcatcgtc
P6	gcgcTCTAGAaacgacgatccttcaaagaa
P7	CCGCGGATCCctagctttgaagacggcgg
P8	cgGGATCCttcacgtgaaacatgcagct
P9	tcgttcatgggttcatcctgacgcaat
P10	gatgaacccatgaacgacgatccttcaaaga
P11	gcTCTAGActagctttgaagacggcgg
P12	ccagaagcgttagactgcc
P13	gctcaccattctatcttcctcaaaccggc
P14	gcgcTCTAGAgctcggaagaacatattcg
P15	CCGCGGATCC ttaaccctgatcgtttttga
P16	gcTCTAGAaaactttcgccattcaaattt
P17	cgGGATCCccaaggtgaaatcgtggc
P18	gcTCTAGAtgtttttcaccacgccaa
P19	cgGGATCCgaggttgaaaagcgtggtg
P20	ttccgatctccacgccat
P21	tccggtggccgaccgTCTAGAaggctatgacgttcaaggaaaagg
P22	agacggtcggccaccGGATCCttgagcgcatcgcgaaa
P23	acattcagcgttgcggtca
P24	gcctttctacggcttaacaccag
P25	tccggtggccgaccgTCTAGAgggacatgaggatgctgatg
P26	agacggtcggccaccGGATCCatgccaagatgaccgctagtg
P27	tggctgacatggggattg
P28	cgcaaattctggcaggattat
P29	tccggtggccgaccgTCTAGAggctgtcttttaaggccg
P30	agacggtcggccaccGGATCCgcccgatccggtacttatattc
P31	gacaggtccgcgtctttc
P32	ttgagaaactcgatgccgg
P33	tccggtggccgaccgTCTAGAtcaaaaatggcaaccgcc

P34	agacggtcggccaccGGATCCgagacatgttttaaccagccgg
P35	agattacaatcgacgtcgtttcg
P36	gcTCTAGAatgataataaggaggccatatgtctaaagg
P37	cgGGATCCttaaggcttcggctttttatc
P38	taaggaggccatatgtctaaaggtga
P39	gccgtacgatttatacagctcatgc
P40	ctaGCTAGCatggtgagcaagggcgag
P41	cgcGGATCCctagctttgaagacg
P42	cgcGGATCCttaaccctgatcgttttt
P43	cgGAATTCggcttttgctgaagcgaag
P44	cgGGATCCacgatgcgtaacaagcgc
P45	cgGAATTCtttgcggggaacctga
P46	cgggatccctagtgacggc
P47	cgGAATTCatcctgaaaacggtgcgg
P48	cgGGATCCttcctgatcgtcggtttcg
P49	GGATCCgtgagcaagggcgagga
P50	CTCGAGttacttgtacagctcgtcc
P51	gcgcTCTAGAgctcggctctgcaaacaat

* Restriction sites are shown in uppercase

Supplementary Note 1

IfoP identification and characterization

IfoP is encoded by BMEI1434 from the *Brucella* ORFeome. IfoP was isolated in a previously described screening for new-pole markers in *B. abortus* [8]. Indeed the IfoP-YFP fusion carried by a pRH005 [9] derivative localizes, in ~80-90% of the bacteria, as a fluorescent focus at the pole opposite to PdhS-mCherry (Supplementary Fig. 4a-d). Time lapse experiments and demographs (Supplementary Fig. 4c,g) showed that IfoP is delocalized in predivisional cells (in about 10% of the bacteria), and relocalized in a focus at the end of the constriction. IfoP is thus a reliable marker of new poles. An IfoP-CFP fusion displayed a subcellular localization similar to IfoP-YFP (Supplementary Fig. 4e-h).

Supplementary Methods

To construct plasmid pXDB007 (allelic replacement of *parB* with *mcherry-parB*), upstream region of *parB* was PCR amplified using primers (P1 + P2) from *Brucella abortus* 544 genomic DNA. The *mcherry* coding sequence was amplified from pMT688 [10] using primers (P3 + P4) for six cycles. After these six first cycles, primer P5 was added for 30 cycles with an increase of 2°C of the hybridization temperature. A joint PCR between amplification products from both previous PCR was performed using primers (P1 + P5), and the product was inserted into an *Eco*RV-linearized pGEM®-T (Promega). The resulting plasmid, pGEM®-T t*parA-mcherry* was checked by sequencing. The *parB* coding sequence was amplified by PCR with P6 + P7 primers on *Brucella abortus* 544 genomic DNA and the product was inserted into pGEM®-T, checked by sequencing. The *parB* coding sequence was excised from this recombinant plasmid using *Xba*I and *Bam*HI before its ligation with pGEM®-T t*parA-mcherry* linearized by the same enzymes. Thereafter, the final t*parA-mcherry-parB* sequence was excised with *Spe*I and *Bam*HI and ligated into the pNPTS138 plasmid cut with the same enzymes.

The same primers were used to create the pNPTS138-t*parA-yfp-parB* since P3 and P4 primers also allow amplification of the *yfp* coding sequence.

pXDB008 (for integration of a fusion between the *gidA* promoter and the *parB* coding sequence at the *parB* locus) was constructed by a joint PCR between *gidA* promoter sequence (amplicon obtained with P8 + P9 primers) and *parB* amplification product (obtained with P10 + P11 primers) using primers P8 and P11. The amplification product was then transferred into a pSK *ori*T *kan* vector using *Xba*I and *Bam*HI restriction enzymes for the insertion of the P*gidA-parB* fusion.

A similar strategy for the construction of pXDB007 was performed for pXDB016 (allelic replacement of *repB* with *yfp-repB*) generation. Briefly, primers P12 and P13 were used to

amplify the upstream region of *repB* (P*repABC-repA*). The amplification product was attached by joint PCR to the *yfp* coding sequence generated by the same way as *mcherry* (see pXDB007 construct) from pMT521 [10] using the same primers and inserted into *Eco*RV-linearized pGEM®-T. The resulting plasmid, pGEM®-T P*repABC-repA-yfp*, was checked by sequencing. The *repB* coding sequence was amplified with primers P14 + P15 and inserted into pGEM®-T vector. The *repB* coding sequence was then excised from this recominant plasmid using *Xba*I and *Bam*HI, before its ligation with pGEM®-T P*repABC-repA-yfp* linearized by the same enzymes. Thereafter, the final P*repABC-repA-yfp-repB* fragment was excised with *Spe*I and *Bam*HI and ligated into the pNPTS138 plasmid cut with the same enzymes, generating pXDB016.

Plasmid pKS *ori*T *cat* $parS_{P1}$ (pXDB024) was constructed by the amplification of $parS_{P1}$ sequence from the pFHC-3212 plasmid [11] using primers P16 + P17, the PCR product was inserted into an *Eco*RV-restricted pGEM®-T plasmid and then excised using *Bam*HI and *Xba*I before its ligation with a pKS *ori*T *cat* plasmid restricted with the same enzymes. A similar strategy was used to create the pKS *ori*T *cat* $parS_{pMT1}$ plasmid (pXDB025) but using primers P18 and P19 instead of P16 and P17.

In order to minimize the perturbations of the insertions of *parS** (from either P1 or pMT1) sites on the expression of neighboring genes, we choose to integrate *parS** sites in regions characterized with head-to-head orientation genes, as close as possible to the predicted *oriI*, *terI*, *oriII* and *terII* regions. Plasmid pXDB010 (allelic replacement allowing insertion of $parS_{P1}$ near *oriI*, *NoriI*, see Supplementary Figure 2f) was constructed by amplifying the upstream *oriI* region from genomic DNA using P20 and P21 primers and the downstream region with P22 and P23 primers. A joint PCR was performed using P20 and P23 primers in order to associate both amplification products, and the final amplicon was transferred into pGEM®-T vector for sequencing. The $parS_{P1}$ sequence was excised from plasmid pKS *ori*T

cat parS$_{P1}$ (pXDB024) cut by *Bam*HI and *Xba*I and ligated into pGEM®-T *oriI* linearized with the same enzymes. The final *oriI*$_{P1}$ fragment (*parS*$_{P1}$ in the cloned *NoriI* region) was excised from pGEM®-T *oriI parS*$_{P1}$ with *Spe*I and *Bam*HI and subsequently ligated with pNPTS138 vector digested with these enzymes.

The same strategy was used for the construction of allelic replacement plasmids pXDB011 (for the insertion of *parS*$_{pMT1}$ at *NoriI*), pXDB012 (for the insertion of *parS*$_{P1}$ at *NterI*), pXDB018 (for the insertion of *parS*$_{pMT1}$ at *NoriII*), pXDB019 (for the insertion of *parS*$_{P1}$ at *NterII*) and pXDB021 (for the insertion of *parS*$_{P1}$ at *NoriII*), using P24+P25 and P26+P27 coupled primers for the upstream and downstream region of *NterI* (see Supplementary Figure 2f); P28+P29 and P30+P31 for the upstream and downstream region of *NoriII* and P32+P33 and P34+P35 for the upstream and downstream region of *NterII* (see Supplementary Figure 4e).

Plasmid pXDB014 was constructed from the amplification of *yfp-parB*$_{pMT1}$ fusion from pMS319 [12] using P38 and P39 primers. The amplicon was inserted into pGEM®-T vector at the *Eco*RV site. This recombinant plasmid was then digested by *Hin*dIII and *Xba*I and the excised insert was ligated into pMR *kan* restricted with the same enzymes.

For the construction of pXDB015 plasmid, the *cfp-parB*$_{P1}$ fusion was amplified from pFHC2896 [11] using P36 and P37, and the amplicon was inserted into a pBBR1 MCS1 plasmid at the *Eco*RV site. This recombinant plasmid was then restricted with *Xba*I and *Bam*HI enzymes and the excised insert was ligated into pMR *kan* digested with the same enzymes.

Plasmid pXDB013 was constructed by performing a triple ligation involving both *yfp-parB*$_{pMT1}$ and *cfp-parB*$_{P1}$ fusions excised from their respective pXDB014 and pXDB015 vectors with *Hin*dIII/*Xba*I and *Xba*I/*Bam*HI respectively, and ligated in pMR *kan* digested with *Hin*dIII and *Bam*HI.

Plasmid pXDB022 was generated by the excision of the *yfp-parB*$_{pMT1}$ *cfp-parB*$_{P1}$ fragment using *Hin*dIII and *Bam*HI from pXDB013, that was subsequently ligated into a pMR *nours* digested with the same enzymes.

Plasmids pXDB002 and pXDB003 were constructed by PCR using primers P40 + P41 on pNPTS138-t*parA-yfp-parB* and P40 + P42 on pXDB016, respectively. Amplification products were cloned into pGEM®-T vector for sequencing, and the inserts were excised by *Nhe*I and *Bam*HI and ligated into pBBR-IBA3plus [13] digested with *Xba*I (compatible with *Nhe*I) and *Bam*HI.

Plasmids pXDB004, pXDB005 and pXDB006 were constructed by PCR amplification with primers P43 + P44, P45 + P46 and P47 + P48, respectively. Each amplicon was transferred into pLAU43 using *Eco*RI and *Bam*HI digestion sites. Fragments containing the *lacO* array linked to *parS1-2*, *repS1* or *repS2* were excised from recombinant pLAU43 with *Eco*RI and *Xba*I and transferred into the pPR9TT digested by the same enzymes.

Plasmid pKS *ori*T *cat mcherry* (pXDB027) was constructed by amplification of the *mcherry* gene with P49 + P50, digestion of the amplicon with *Xba*I and *Bam*HI and cloning in a pKS *ori*T *cat* vector.

The *popZ* gene (predicted promoter and coding sequence) was amplified with P51 and P52 primers in order to construct pKS *ori*T *cat popZ-mcherry* (pXDB017). The PCR product was first ligated into pGEM®-T vector for sequencing and the insert was subsequently excised with *Xba*I and *Bam*HI enzymes and ligated with a pKS *ori*T *cat mcherry* digested with the same enzymes.

Supplementary References

1. de Barsy M, *et al.* Identification of a *Brucella* spp. secreted effector specifically interacting with human small GTPase Rab2. *Cellular microbiology* **13**, 1044-1058 (2011).

2. Simon R, Priefer U, Pühler A. A broad host range mobilization system for *in vivo* genetic engineering: transposon mutagenesis in Gram negative bacteria. *Nature Biotechnology* **1**, 784-791 (1983).

3. Van der Henst C, *et al.* Overproduced *Brucella abortus* PdhS-mCherry forms soluble aggregates in *Escherichia coli*, partially associating with mobile foci of IbpA-YFP. *BMC microbiology* **10**, 248 (2010).

4. Lau IF, Filipe SR, Soballe B, Okstad OA, Barre FX, Sherratt DJ. Spatial and temporal organization of replicating *Escherichia coli* chromosomes. *Molecular microbiology* **49**, 731-743 (2003).

5. Santos PM, Di Bartolo I, Blatny JM, Zennaro E, Valla S. New broad-host-range promoter probe vectors based on the plasmid RK2 replicon. *FEMS microbiology letters* **195**, 91-96 (2001).

6. Haine V, *et al.* Systematic targeted mutagenesis of *Brucella melitensis* 16M reveals a major role for GntR regulators in the control of virulence. *Infection and immunity* **73**, 5578-5586 (2005).

7. Kovach ME, *et al.* Four new derivatives of the broad-host-range cloning vector pBBR1MCS, carrying different antibiotic-resistance cassettes. *Gene* **166**, 175-176 (1995).

8. Dotreppe D, Mullier C, Letesson JJ, De Bolle X. The alkylation response protein AidB is localized et the new poles and constriction sites in *Brucella abortus*. *BMC microbiology* **11**, 257 (2011).

9. Hallez R, Letesson JJ, Vandenhaute J, De Bolle X. Gateway-based destination vectors for functional analyses of bacterial ORFeomes: application to the Min system in *Brucella abortus*. *Appl Environ Microbiol* **73**, 1375-1379 (2007).

10. Thanbichler M, Iniesta AA, Shapiro L. A comprehensive set of plasmids for vanillate- and xylose-inducible gene expression in *Caulobacter crescentus*. *Nucleic Acids Res* **35**, e137 (2007).

11. Nielsen HJ, Ottesen JR, Youngren B, Austin SJ, Hansen FG. The *Escherichia coli* chromosome is organized with the left and right chromosome arms in separate cell halves. *Molecular microbiology* **62**, 331-338 (2006).

12. Toro E, Hong SH, McAdams HH, Shapiro L. *Caulobacter* requires a dedicated mechanism to initiate chromosome segregation. *Proceedings of the National Academy of Sciences of the United States of America* **105**, 15435-15440 (2008).

13. Thanbichler M, Shapiro L. MipZ, a spatial regulator coordinating chromosome segregation with cell division in *Caulobacter*. *Cell* **126**, 147-162 (2006).